

FZD5 regulates cellular senescence in human mesenchymal stem/stromal cells

Seiko Harada¹ | Yo Mabuchi^{1,2,3} | Jun Kohyama¹  | Daisuke Shimojo¹ | Sadafumi Suzuki¹ | Yoshimi Kawamura^{1,4} | Daisuke Araki¹ | Takashi Suyama⁵ | Masunori Kajikawa⁶ | Chihiro Akazawa^{2,7} | Hideyuki Okano¹  | Yumi Matsuzaki^{1,5}

¹Department of Physiology, Keio University School of Medicine, Tokyo, Japan

²Department of Biochemistry and Biophysics, Graduate School of Medical and Dental Sciences, Tokyo Medical and Dental University, Tokyo, Japan

³Department of Haematology, University of Cambridge, Cambridge, UK

⁴Department of Aging and Longevity Research, Faculty of Life Sciences, Kumamoto University, Kumamoto, Kumamoto, Japan

⁵Department of Life Science, Shimane University Faculty of Medicine, Izumo, Shimane, Japan

⁶Medical & Biological Laboratories Co, Ltd, Nagoya, Aichi, Japan

⁷Intractable Disease Research Centre, Juntendo University School of Medicine, Tokyo, Japan

Correspondence

Hideyuki Okano, MD, PhD, Department of Physiology, Keio University School of Medicine, 35 Shinanomachi, Shinjuku-ku, Tokyo 160-8582, Japan.
Email: hidokano@a2.keio.jp

Yumi Matsuzaki, MD, PhD, Department of Life Science, Shimane University Faculty of Medicine, 89-1 Enya-cho, Izumo, Shimane 693-8501, Japan.
Email: matsuzak@med.shimane-u.ac.jp

Funding information

Japan Agency for Medical Research and Development, Grant/Award Number: 18bm0404022h0001; Ministry of Education, Culture, Sports, Science and Technology, Grant/Award Numbers: JP18KK0449, JP19K10024, JP19KK0216; Takeda Medical Research Foundation; Japan Society for the Promotion of Science (JSPS)

Abstract

Human mesenchymal stem/stromal cells (hMSCs) have garnered enormous interest as a potential resource for cell-based therapies. However, the molecular mechanisms regulating senescence in hMSCs remain unclear. To elucidate these mechanisms, we performed gene expression profiling to compare clonal immature MSCs exhibiting multipotency with less potent MSCs. We found that the transcription factor Frizzled 5 (*FZD5*) is expressed specifically in immature hMSCs. The *FZD5* cell surface antigen was also highly expressed in the primary MSC fraction (LNGFR⁺THY-1⁺) and cultured MSCs. Treatment of cells with the *FZD5* ligand WNT5A promoted their proliferation. Upon *FZD5* knockdown, hMSCs exhibited markedly attenuated proliferation and differentiation ability. The observed increase in the levels of senescence markers suggested that *FZD5* knockdown promotes cellular senescence by regulating the noncanonical Wnt pathway. Conversely, *FZD5* overexpression delayed cell cycle arrest during the continued culture of hMSCs. These results indicated that the intrinsic activation of *FZD5* plays an essential role in negatively regulating senescence in hMSCs and suggested that controlling *FZD5* signaling offers the potential to regulate hMSC quality and improve the efficacy of cell-replacement therapies using hMSCs.

KEYWORDS

aging, *FZD5* receptor, human, mesenchymal stem/stromal cells, senescence

Seiko Harada and Yo Mabuchi contributed equally to this study.

This is an open access article under the terms of the Creative Commons Attribution-NonCommercial License, which permits use, distribution and reproduction in any medium, provided the original work is properly cited and is not used for commercial purposes.

©2020 The Authors. STEM CELLS published by Wiley Periodicals LLC on behalf of AlphaMed Press 2020

1 | INTRODUCTION

Mesenchymal stem/stromal cells (MSCs) are typically defined as multipotent mesenchymal stromal cells present in the bone marrow (BM) and other organs.^{1,2} These cells are characterized by their spindle-shaped morphology and capacity for self-renewal and differentiation into cells of mesenchymal lineages.³ MSCs were originally isolated from BM cells by exploiting their adherence to plastic substrates. However, long-term culture in vitro leads to replicative senescence of MSCs.⁴⁻⁶ Senescence is a cellular condition characterized by irreversible cell cycle arrest and high activation of senescence-related markers (genes and proteins); increased gene expression and senescence-related β -galactosidase (SA β -gal) activity, such as P53, P16, and P21, are the main features of cellular senescence.^{7,8} Replicative senescence results in an increase in the cell area, changes the metabolic phenotype, and impairs multi-differentiation capacity.⁹⁻¹² It has also been reported to inhibit therapeutic activity, including reduced anti-inflammatory cytokine production and reduced fracture repair capacity.¹³⁻¹⁵ Therefore, replicative senescence can be a significant barrier to the development of cell therapy technologies for applications in regenerative medicine.¹⁶⁻¹⁸

The Wnt signaling pathway is an important pathway that determines cell fate.¹⁹ Activation levels of the β -catenin signaling pathway have been reported to be closely associated with the maintenance of undifferentiated stem cells.²⁰⁻²² Moreover, the over-activation of the β -catenin signaling pathway has been shown to cause senescence of HSCs.²³⁻²⁵ Various other factors, such as stimulation by inflammatory cytokines, cell-to-cell contact, and dysregulation of intracellular signaling pathways, promote cell senescence.^{26,27} Thus, the analysis of signals that affect human MSCs (hMSCs) may contribute to our understanding of the mechanisms of MSC senescence.

The heterogeneity of MSC populations makes it difficult to identify MSC-specific signals. Even if the criteria for defining MSCs, including (a) their plastic-adherent characteristics in standard culture conditions, (b) expression of particular subsets of cell surface markers, and (c) the differentiation capability to osteoblasts, adipocytes, and chondroblasts in vitro, as proposed by the International Society for Cellular Therapy are met, there is no guarantee that the MSC population is homogeneous.²⁸ Heterogeneous, nonclonal cultures of stromal cells exhibit diverse differentiation and proliferative capacities.²⁹ In our previous studies, we used a suite of cell surface markers to ensure quality and clonality.^{30,31} We found that the LNGFR⁺ (CD271) THY-1⁺ (CD90) fraction isolated from adult human BM, synovium, dental pulp, or induced pluripotent stem cell-derived cells contained a high proportion of hMSCs.^{30,32-34} Moreover, based on the results of single-cell sorting and clonal expansion of LNGFR⁺THY-1⁺ cells, we concluded that rapidly expanding clones (RECs) exhibited various properties associated with an immature phenotype. In particular, RECs, in addition to being the most expandable population among the isolated clones, could differentiate into the three mesenchymal lineages from a single cell.

In this study, we performed extensive gene expression profiling to identify the molecular mechanisms underlying the differences between clonal immature MSCs and less potent clonal MSCs. We found that Frizzled5 (*FZD5*) was expressed specifically in the highly functional and immature hMSC cells. Conversely, knockdown of

Significance statement

Mesenchymal stem/stromal cells (MSCs) hold considerable promise for cell therapy. Generally, MSCs are cultured in vitro to increase cell numbers and ensure functionality. However, long-term culture can lead to cellular senescence, wherein cells no longer replicate. Here, the clones derived from single MSCs were evaluated, revealing that the *FZD5* regulatory protein is specifically expressed in highly functional MSCs. *FZD5* prevents senescence and preserves multipotency in the most immature, rapidly proliferating subtype of MSCs. Controlling *FZD5* gene expression may thus allow the suppression of MSC senescence, while maintaining their stem cell properties throughout long-term culture in vitro.

FZD5 resulted in the loss of stem cell properties, whereas *FZD5* over-expression inhibited senescence in hMSCs. These findings provide evidence that *FZD5* plays a key role in regulating hMSC properties, including the maintenance of proliferation and multilineage potency.

2 | MATERIALS AND METHODS

2.1 | Cell preparation and fluorescence-activated cell sorting (FACS)

All BM-MNC experiments were performed using Poietics BM-MNCs purchased from LONZA. Ethical approval for the generation of these cells was comprehensively undertaken by LONZA. hMSCs were prepared from human BM (human BM-MNCs; Lonza, Amagasaki, Japan) as described in our previous report and in the Supplemental Experimental Procedures.^{30,35} All experimental protocols were approved by the animal committee of Keio University, Japan. All methods were conducted in strict accordance with the approved guidelines of the institutional animal care committee. LNGFR-PE (Miltenyi Biotec, Bergisch-Gladbach, Germany) and THY-1-APC (BD Pharmingen, San Jose, California) were added to the human BM cells and incubated for 30 minutes on ice. The tube was centrifuged, the supernatant was discarded, and HBSS containing propidium iodide (Sigma, St. Louis, Missouri) was added. The cells were sorted using a triple-laser MoFlo (Beckman Coulter, Brea, California), FACS Vantage SE, or FACS Aria III (Becton Dickinson, Bedford, Massachusetts). The data were analyzed using FlowJo software (Tree Star, Ashland, Oregon). All flow cytometry experiments are described in the Supplemental Experimental Procedures.

2.2 | Cell culture and immunocytochemistry

hMSCs were cultured in DMEM (Nacalai Tesque, Kyoto, Japan) containing 20% fetal bovine serum (FBS), 10 mM HEPES (Nacalai Tesque),

10 ng/mL basic fibroblast growth factor (recombinant human FGF-basic; Peprotech, Rocky Hill, New Jersey), and 1% penicillin-streptomycin (Nacalai Tesque). Wnt treatment was performed in DMEM containing 1% FBS, 10 mM HEPES, and 1% penicillin-streptomycin. All cell culture experiments are described in the Supplemental Experimental Procedures.

The cells were plated on eight-well chamber slides (Iwaki) or glass slips (Matsunami) coated with poly-L-ornithine (Sigma) and fibronectin (Sigma). After several treatments and culture, the cells were fixed (4% PFA) and blocked with phosphate-buffered saline containing 5% FBS. F-actin was stained with Alexa fluor 555 Phalloidin (Molecular probes). We prepared the anti-FZD5 (#6F5B9) and anti-ROR2 (#6F12A2) monoclonal antibodies in Medical & Biological Laboratories Co, Ltd (previously named ACTGen, Inc) (antibody information, Table S2). The proximity-ligation assay (PLA) visualizes the interaction when a pair of oligonucleotide probes are close to each other. For this assay, the Duolink in situ kit was used according to the manufacturer's protocol (Olink Bioscience). To detect the interaction between non-canonical Wnt pathway-related factors (FZD5/ROR2), the in situ PLA was performed with RECs cultured in 1% serum. The number of dots was counted as signals. A signal is generated and interaction is detected only when the target protein is within 40 nm of each other. In each assay, an average of more than 200 cells was scored. All immunocytochemistry experiments are described in the Supplemental Experimental Procedures.

2.3 | Gene expression and Microarray analysis

Total RNA was extracted from hMSC clones (RECs, moderately expanding clones [MECs], and slowly expanding clones [SECs]). After purification, 300 ng of total RNA was labeled with Cy3 and hybridized to an Agilent human whole-genome chip (4 × 44 K, AMADID = 14 850; Agilent Technologies, Santa Clara, California), which was scanned using a microarray scanner system (Agilent Technologies). Gene expression analysis was performed using GeneSpring GX10 (Agilent Technologies). The results were uploaded to the Gene Expression Omnibus (number: GSE86369). The quantitative PCR was performed with fast SYBR Green master mix or Power SYBR Green PCR master mix (Life Technologies) and an HT7900 fast real-time PCR system or a ViiA7 real-time PCR system (Applied Biosystems) (Table S1). Microarray and quantitative PCR analyses are described in the Supplemental Experimental Procedures.

2.4 | FZD5 knockdown and overexpression

Knockdown of FZD5 was performed using the lentiviral vectors CS-shFZD5-EG and CS-shFZD5-EF-mRFP (Table S1). hMSCs were seeded on six-well plates at a density of 2×10^5 cells/well. After approximately 24 hours, appropriate amounts of CS-shFZD5-EG or CS-shFZD5-mRFP lentivirus were added. Following incubation for 12 hours, the medium containing lentivirus was removed and the cells were passaged if necessary. Four days after viral infection, EGFP-

positive or mRFP-positive hMSCs were isolated by FACS. Ten days after viral infection, several analyses were performed.³⁶ FZD5 was overexpressed using the PiggyBac transposon vector system (System Biosciences, Palo Alto, California). Wild-type (wt)-FZD5 (PB513-FZD5-2xHA) or mutant (mut)-FZD5 (PB513-FZD5mut-2xHA) was transfected into hMSCs along with the PB200 vector (System Biosciences) at a molar ratio of 5:1 using the Human MSC Nucleofector Kit (Amaxa Biosystems, Cologne, Germany) or ViaFect Transfection Reagent (Promega, Madison, Wisconsin).

2.5 | Statistical analysis

Quantitative data are presented as the means ± SEM from representative experiments ($n \geq 3$). For statistical analyses, the data were evaluated using the Student's *t* test; *P* values <.05 were considered significant.

3 | RESULTS

3.1 | FZD5 is specifically expressed in multipotent hMSCs

In our previous study, we demonstrated that clones resulting from colony-forming hMSCs, which constitute a heterogeneous population, could be classified as RECs, MECs, or SECs based on their capacities (Figure S1A).³⁰ The RECs exhibited robust multilineage differentiation and self-renewal potency. To investigate the molecular mechanisms underlying the behavior of these cells, we isolated RECs and less potent MSCs (MECs or SECs) and analyzed their gene expression profiles. We validated the expression levels of genes whose expression levels in RECs were at least one-fold to two-fold higher than those in MECs/SECs by parsing and clustering the differentially expressed genes (57 genes) using the *k*-means algorithm (Figure S1B,C). Gene expression and ontology analysis revealed that genes upregulated in RECs included Wnt signaling genes involved in the Wnt/Ca⁺, PCP, and Wnt/β-catenin signaling pathways (Figure S1D). Therefore, we focused on the Wnt-Fzd pathway in our subsequent characterization of RECs.

Among the FZD family of genes, FZD5 was found to be specifically expressed in RECs (Figure 1A) and was confirmed by quantitative RT-PCR to be the most upregulated gene in RECs compared with MECs/SECs (Figure 1B). Western blotting and immunocytochemistry also confirmed the specific expression of FZD5 in RECs at the protein level (Figure 1C,D). To investigate the expression of FZD5 in primary cells and eliminate the effect of culture conditions, we examined freshly isolated cell fractions from human BM and found that FZD5 was expressed only in the LNGFR⁺THY-1⁺ MSC fraction (Figure 1E,F). The *Fzd5* mRNA expression level was also elevated in purified mouse MSCs (Figure S2). Together, these data indicated that FZD5 is specifically expressed in highly potent and freshly isolated MSCs. To ascertain whether FZD5 plays an important role in maintaining multipotency, we focused on the function in RECs.

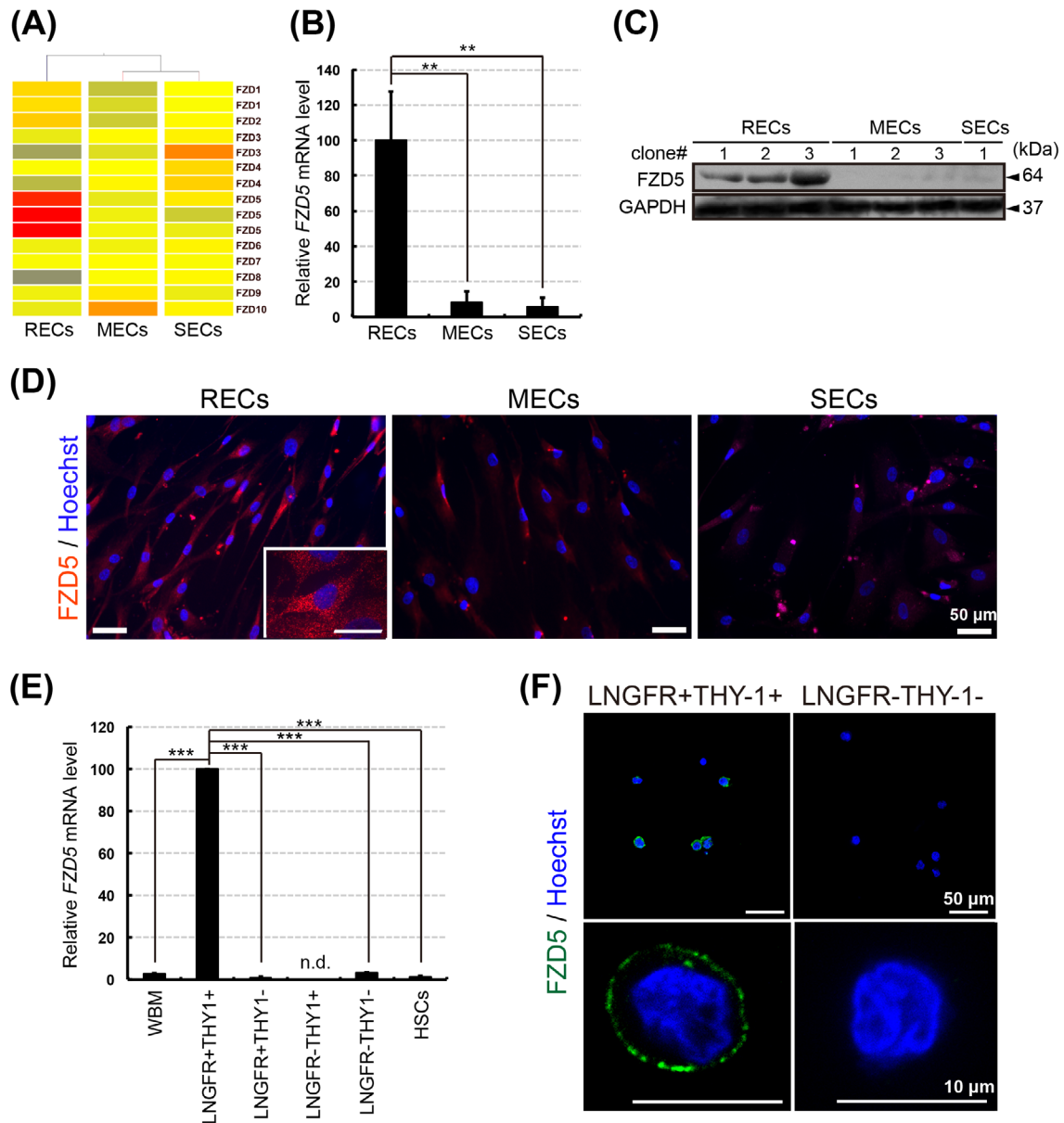


FIGURE 1 FZD5 is specifically expressed in immature mesenchymal stem/stromal cells (MSCs). A, Heat map of FZD family gene expression in rapidly (RECs), moderately (MECs), and slowly (SECs) expanding clones (repeated gene names indicate results from different probe sets). B, Relative FZD5 expression levels in RECs, MECs, and SECs as determined by quantitative RT-PCR. The ratios of FZD5 to GAPDH mRNA were calculated for three clones of each cell type ($n = 3$). The mean level in three RECs was adjusted to 100. C, Western blot analysis of FZD5 in RECs, MECs, and SECs. GAPDH was used as the internal control. D, Immunostaining of FZD5 (red) and nuclei (blue) in RECs, MECs, and SECs. E, Relative FZD5 mRNA expression level in each fraction of bone marrow mononuclear cells. FZD5 mRNA expression levels were normalized against the corresponding levels of GAPDH mRNA. Human whole bone marrow (WBM) cells were used as an unsorted cell population. Hematopoietic stem cells (HSCs) were sorted to obtain the CD34⁺THY1⁺ population. The mean level in the three LNGFR⁺THY1⁺ clones was adjusted to 100. Three clones of each cell type were used ($n = 3$). n.d., not detected. F, Immunostaining of FZD5 (green) and nuclei (blue) in freshly sorted cells of the LNGFR⁺THY1⁺ or LNGFR⁻THY1⁻ fraction from human bone marrow. Data are presented as the means \pm SEM. ** $P < .01$, *** $P < .001$; Student's *t* test

3.2 | Multipotent hMSCs can be activated by the FZD5-related pathway

The Wnt pathway is classified into canonical and noncanonical modes of activity.³⁷ In the canonical pathway, Wnt ligands bind to cognate FZD receptors along with a coreceptor, lipoprotein receptor-related

protein 5/6 (LRP5/6). The AXIN2 gene, a direct downstream target, is expressed in many sites in which Wnt signaling is active. To determine whether these factors function in conjunction with FZD5 in RECs, we measured expression levels of the corresponding genes (qRT-PCR, AXIN2, LRP5, and LRP6), β -catenin dephosphorylation as shown using the anti-active β -catenin 8E7 antibody, and activation of the canonical

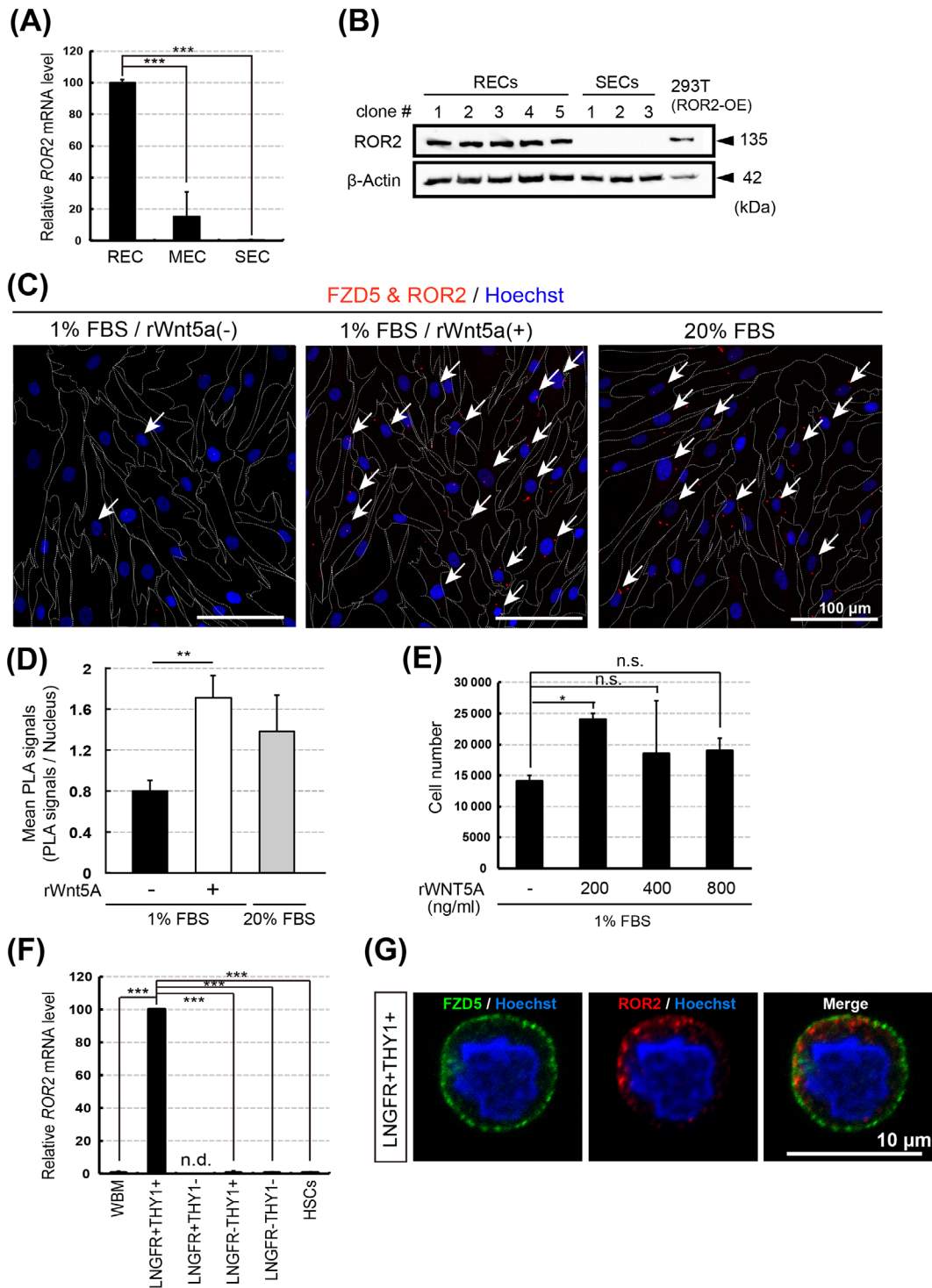


FIGURE 2 The noncanonical Wnt pathway can activate mesenchymal stem/stromal cell (MSC) proliferation. A, Relative ROR2 expression levels in rapidly (RECs), moderately (MECs), and slowly (SECs) expanding clones (quantitative RT-PCR). ROR2/GAPDH mRNA ratios were calculated for three clones of each cell type ($n = 3$). The mean level in three RECs was adjusted to 100. B, Western blot analysis of ROR2 in RECs and SECs. GAPDH served as the internal control. C, FZD5 and ROR2 colocalization (in situ PLA analysis). The white arrows indicate the cells in which the signal was detected. Dotted lines indicate cell boundaries. D, Quantification of FZD5-ROR2 interaction in RECs, determined by PLA signal number per cell; $n = 3$ clones. E, REC proliferation in the presence of rWnt5A. Cells were seeded (1×10^4) and counted after 1 week; $n = 3$ clones. F, Relative ROR2 expression levels in freshly sorted bone marrow mononuclear cells. Human WBM cells served as an unsorted cell population. HSCs were sorted into the CD34⁺THY1⁺ population. ROR2/GAPDH mRNA ratios were calculated as in (A) ($n = 3$); LNGFR⁺THY1⁺ mean levels were adjusted to 100. G, FZD5 (green), ROR2 (red), and nuclei (blue) immunostaining in freshly sorted LNGFR⁺THY1⁺ BM-MNCs. Data represent the means \pm SEM. n.s., not significant. * $P < .05$, ** $P < .01$, *** $P < .001$; Student's t test

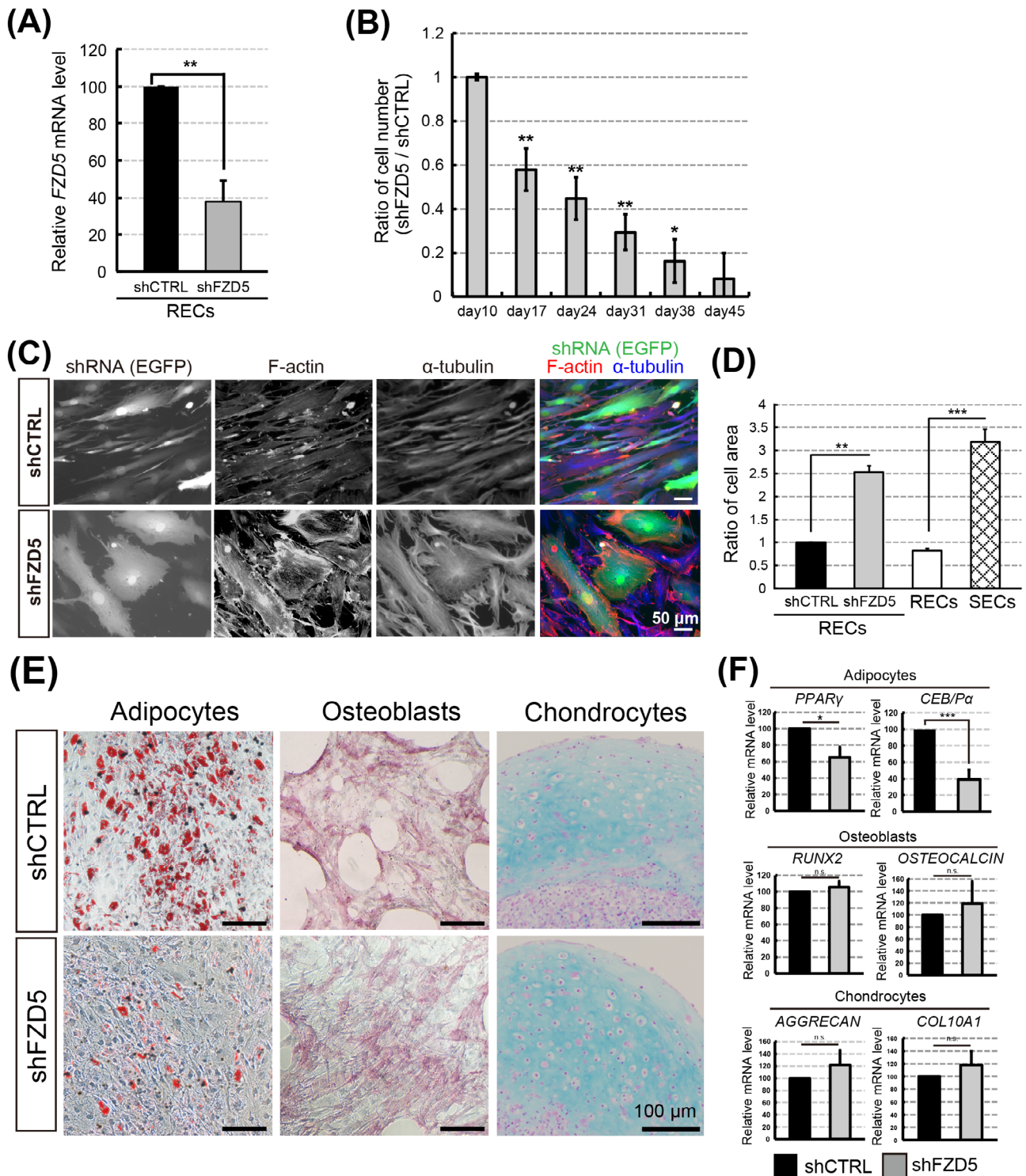


FIGURE 3 FZD5 knockdown increases mesenchymal stem/stromal cell (MSC) cell size and decreases their adipogenic differentiation potential and proliferative capacity. A, Relative FZD5 expression levels in rapidly expanding clones (RECs) transfected with shFZD5 or control (shCTRL) lentivirus. FZD5 mRNA levels were normalized to GAPDH. Three clones of each cell type were used ($n = 3$). B, Time-dependent changes in shFZD5-transfected REC numbers. Ratio of the number of shFZD5 cells divided by the number of shCTRL cells is shown. The mean at day 10 (after transfection) was adjusted to 1; $n = 3$ clones. C, F-actin (red) and α -tubulin (blue) immunostaining in RECs transfected with shCTRL or shFZD5 plus the EGFP expression vector (green). Scale bar = 50 μ m. D, Quantification of cell areas. The mean size of shCTRL-treated cells was defined as 1; $n = 3$ clones. E, Adipogenic, osteogenic, or chondrogenic differentiation capacities of shCTRL- or shFZD5-transfected RECs. Cells were stained as follows: adipocytes (Oil Red-O), osteoblasts (ALP), and chondrocytes (Alcian blue). Scale bar = 100 μ m. F, Relative expression of adipocyte (*PPAR γ* and *C/EBP α*), osteoblast (*RUNX2* and *OSTEOCALCIN*), and chondrocyte (*AGGRECAN* and *COL10A1*) markers in cells derived from shFZD5- or shCTRL-treated RECs. The mean level in shCTRL-treated cells was adjusted to 100; $n = 3$ clones. Data represent the means \pm SEM. n.s., not significant. * $P < .05$, ** $P < .01$, *** $P < .001$; Student's *t* test

Wnt pathway as estimated using the TOP/FOP flash assay (Figure S3A-E). According to these results, the canonical Wnt pathway seemed to be activated in RECs, albeit not statistically significant. Focusing on the ligands of FZD5, we found that recombinant WNT3A

promoted the activation of the canonical Wnt pathway. However, WNT5A, which is primarily involved in the noncanonical pathway, did not cross-activate but instead inhibited the canonical Wnt pathway (Figure S3F).

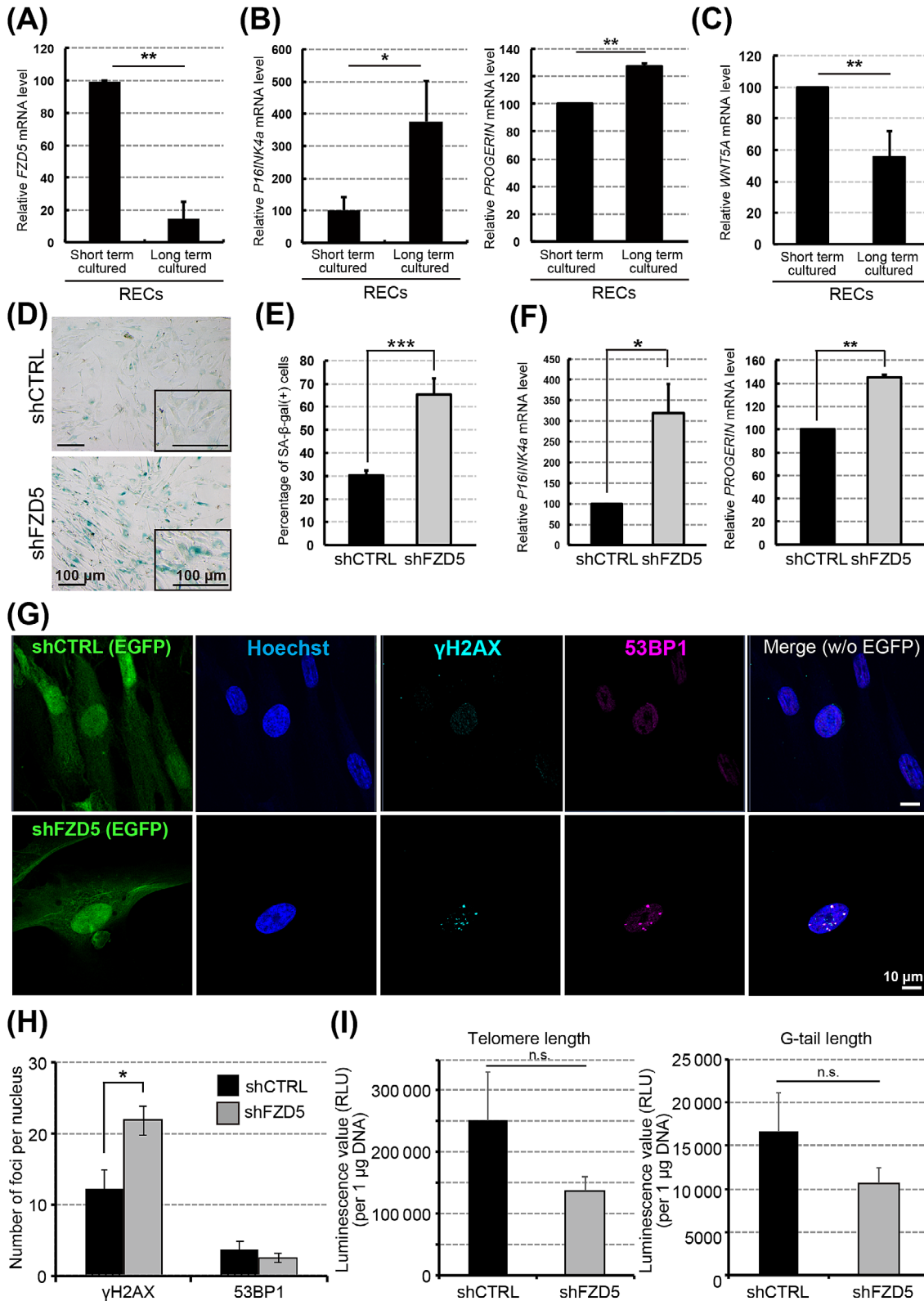


FIGURE 4 Legend on next page.

In the noncanonical Wnt pathway, ROR2 functions as a coreceptor of FZDs.³⁸ ROR2 mRNA expression was fivefold higher in RECs than in MECs, but was undetectable in SECs (Figure 2A). Similarly, in Western blots, ROR2 could be detected in RECs but not in SECs (Figure 2B). Therefore, to determine whether noncanonical Wnt signaling is activated in the RECs, we investigated if there is a direct interaction between FZD5 and ROR2 in the presence of WNT5A using in situ PLA, an assay that can detect the interaction and localization of endogenous proteins with high sensitivity. We confirmed that the PLA could detect the interaction between FZD5 and ROR2 in cells (white arrow), and found that the number of PLA signals was significantly increased upon treatment with recombinant (r)WNT5A (Figure 2C,D). In addition, during ex vivo expansion, the addition of rWNT5A (200 ng/mL) induced REC proliferation (Figure 2E). ROR2 mRNA was expressed in freshly isolated LNGFR⁺THY-1⁺ cells but not in the other populations of BM-MNCs (LNGFR⁻THY-1⁺, LNGFR⁺THY-1⁻, and LNGFR⁻THY-1⁻) (Figure 2F,G). WNT5A was more highly expressed in RECs than in MECs or SECs (Figure S4A). Consistent with this finding, WNT5A mRNA level in the LNGFR⁺THY-1⁺ fraction was higher than those in other fractions (Figure S4B). WNT5A protein was also expressed in RECs grown in culture medium (Figure S4C). Together, these results suggested that the noncanonical Wnt pathway (WNT5A/FZD5/ROR2 axis) is specifically activated in immature hMSCs.

3.3 | Loss of FZD5 impairs MSC stemness

The selective activation of FZD5 signaling in RECs motivated us to investigate the possible role of FZD5-mediated Wnt signaling in the regulation of REC-specific cellular properties. We used a lentiviral vector to introduce a short hairpin RNA (shRNA) targeting FZD5 into RECs (Figure 3A). After culturing the cells, we calculated the numerical ratio of FZD5-knockdown (shFZD5) RECs vs RECs transfected with the control vector (shCTRL), and determined that the proliferation rate in shFZD5-RECs was reduced (Figure 3B). The noncanonical Wnt pathway is deeply involved in stress fiber rearrangement.^{39,40} Therefore, among various REC-specific cellular phenotypes, we initially focused on the finding that F-actin-positive tubular components are rarely detected in RECs (Figure S1). In contrast, FZD5 knockdown triggered stress fiber formation in RECs

(Figure 3C). In addition, shFZD5-RECs exhibited larger cell bodies, resembling those of SECs (Figure 3D). We then investigated the role of FZD5 in the regulation of differentiation potential for mesenchymal lineage. Although osteogenic and chondrogenic differentiation was unaffected, FZD5 knockdown markedly inhibited adipogenic differentiation (Figure 3E). The results of quantitative RT-PCR for lineage-specific marker genes confirmed that FZD5 knockdown in RECs only affected genes associated with adipocyte differentiation, including *PPAR γ* and *C/EBP α* , but not marker genes of osteoblasts (*RUNX2* and *OSTEOCALCIN*) or chondrocytes (*AGGRECAN* and *COL10A1*) (Figure 3F). These findings suggest that, in RECs, FZD5 regulates the capacity to proliferate and differentiate into adipocytes. Notably, shFZD5-RECs exhibit cellular properties similar to those of SECs, the slowest-expanding population with the lowest potential for adipocyte differentiation.

3.4 | FZD5 deletion promotes cellular senescence

Many types of somatic cells undergo senescence when cultured for long periods of time in vitro.⁴¹ To determine whether these phenotypes could also be observed during in vitro senescence, we investigated the expression of *FZD5*, *P16INK4a*, and *PROGERIN* in RECs subjected to short- and long-term culture (fewer than 30 days and more than 60 days, respectively). We found that the expression of *FZD5* decreased with culture duration, whereas that of *P16INK4a* and *PROGERIN* increased (Figure 4A,B). Notably, the expression of *WNT5A* decreased similar to that of *FZD5* (Figure 4C). Upon analyzing the effect of FZD5 knockdown on senescence in RECs, we observed an increased percentage of cells expressing the senescence marker SA- β -gal (Figure 4D,E). We also found that *P16INK4a* and *PROGERIN* were upregulated in shFZD5-RECs (Figure 4F). To comprehensively examine the effects of FZD5 knockdown, we performed RNA sequencing in shFZD5-RECs and shCTRL-RECs. The results showed that the genes involved in senescence and cell cycle (*RB1*, *RB2*, *CBX3*, and *CDK2*) were highly expressed in shFZD5-RECs (Figure S5A). Furthermore, the expression of noncanonical Wnt signaling-related genes (*AP1*, *PLCB1*, *SDC1*, *PRKACA*, and *PRKCA*) tended to decrease (Figure S5B). Western blotting results revealed that the phosphorylation of JNK, p38MAPK, PKC, CaMKII, and ERK in RECs was not higher than that in MECs/SECs (Figure S6A-E). Because the c-JUN phosphorylation was activated in the RECs, it may be involved as a

FIGURE 4 FZD5 knockdown accelerates cellular senescence. A-C, Relative gene expression levels in rapidly expanding clones (RECs) cultured for short (fewer than 30 days) or long (more than 60 days) durations: FZD5 (A), *P16INK4a* and *PROGERIN* (B), and *WNT5A* (C). Three clones of each cell type were used (n = 3). D, SA- β -gal staining of rapidly expanding clones (RECs) transfected with shCTRL or shFZD5. E, Quantification of SA- β -gal-positive cells. Three clones of each cell type were used (n = 3). F, Relative *P16INK4a* and *PROGERIN* mRNA expression levels in RECs transfected with shFZD5 or shCTRL. The mRNA expression levels were normalized against those of *GAPDH* mRNA. The mean level in shCTRL-treated cells was adjusted to 100. Three clones of each cell type were used (n = 3). G, Immunostaining of γ H2AX (light blue) and 53BP1 (red) in RECs transfected with shCTRL or shFZD5 along with EGFP (green). H, Quantification of cell foci (γ H2AX and 53BP1) with shCTRL or shFZD5. I, G-tail telomere hybridization protection assay. The results were calculated as relative light units (RLU) of telomere length and telomere G-tail length per μ g of DNA (n = 3, telomere length, $P = .23$ / G-tail length, $P = .27$). Data represent the means \pm SEM. n.s., not significant. * $P < .05$, ** $P < .01$, *** $P < .001$; Student's t test

target for FZD5-related pathway (Figure S6F). We also found that RAC and CDC42 were activated in response to Wnt5A treatment (Figure S6G,H).

During cellular senescence, the global induction of heterochromatin formation results in the generation of senescence-associated heterochromatic foci. Specifically, phosphorylated H2AX (γ H2AX) recruits DNA-damage-response (DDR)-related factors (eg, 53BP1) to

several hundred kilobase-long regions near the damaged site, where they form large DDR foci.^{42,43} To confirm the progression of senescence in shFZD5-RECs, we examined the expression of γ H2AX and 53BP1 using immunocytochemistry. The results revealed the presence of very few 53BP1 foci and numerous γ H2AX foci in shFZD5-RECs (Figure 4G,H). FZD5 depletion tend to decrease the telomere and G-tail lengths (Figure 4I).

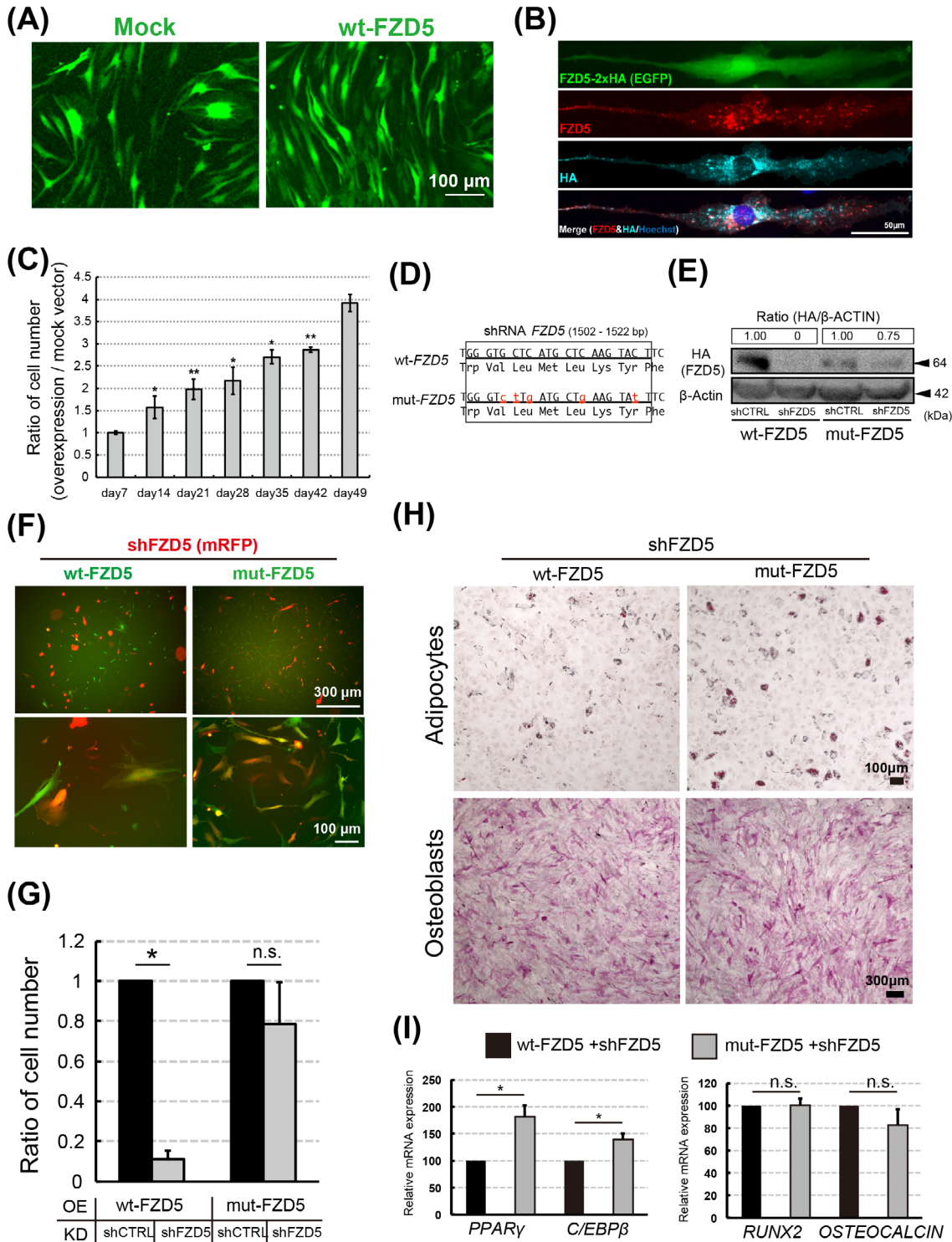


FIGURE 5 Legend on next page.

3.5 | FZD5 overexpression prevents cellular senescence

To analyze the effect of FZD5 signaling on hMSCs, we overexpressed HA-tagged wild-type FZD5 (wt-FZD5) in RECs (Figure 5A). The wt-FZD5 protein could be detected by immunofluorescence using both anti-FZD5 and anti-HA antibodies (Figure 5B). RECs overexpressing wt-FZD5 retained proliferative capacity for longer than controls (Figure 5A,C). To confirm the function of overexpressed FZD5, we performed rescue experiments in shFZD5-RECs. For this purpose, we inserted silent mutations into wt-FZD5 to construct a mutant FZD5 (mut-FZD5) that was not recognized by shFZD5 (Figure 5D). Consequently, mut-FZD5 protein could be detected in REC lysates by Western blotting even when shFZD5 was introduced (Figure 5E). Cells overexpressing wt-FZD5 in the presence of shFZD5 increased in size and became flattened in shape, indicating that the effects of shFZD5 were not rescued by wt-FZD5 (Figure 5F). In contrast, the overexpression of mut-FZD5 in the presence of shFZD5 resulted in the maintenance of cellular size and spindle shape, similar to that in native RECs (Figure 5F). Furthermore, shFZD5 did not affect the proliferation of RECs carrying mut-FZD5, whereas it markedly inhibited the proliferation of RECs expressing wt-FZD5 (Figure 5G).

In the course of the long-term culture (more than 50 days), the adipogenic capacity of shFZD5-RECs persisted under conditions where mut-FZD5 was overexpressed (Figure 5H). Furthermore, the adipogenic differentiation capacity of wt-FZD5 overexpression was reduced (Figure 5H). These observations were confirmed by quantitative PCR of adipocyte (*PPAR γ* and *C/EBP β*) and osteoblast (*RUNX2* and *OSTEOCALCIN*) marker genes (Figure 5I). Together, these data suggested that FZD5 is required to retain both proliferation and differentiation capacity in multipotent MSCs.

4 | DISCUSSION

Extensive attempts have been made to identify surface antigens specific to MSCs; however, the molecular mechanisms regulating the biological features of these cells remained unclear. Previously, we classified populations that retained the multipotent properties of

clonal hMSCs, revealing that RECs constitute the majority of functional MSCs. In the present study, we built on that work, showing that a noncanonical Wnt pathway mediated by FZD5 is involved in regulating the cellular identity in hMSCs. Moreover, because *Fzd5* mRNA expression was also elevated in mouse MSCs, we consider it likely that the role of FZD5 in regulating MSC stemness is evolutionarily conserved.

The role of classical signals in MSCs is very well studied.^{44,45} However, noncanonical Wnt pathway in these cells has not been well characterized. Previous studies evaluated the phenotypes of mice lacking components of non-canonical Wnt pathways, including ROR2 and WNT5A. Deficiencies in both of these factors result in similar phenotypes, including short extremities, short tails, and dyschondroplasia in the distal portion of the extremities.^{46,47} Furthermore, in the human diseases brachydactyly B and recessive Robinow syndrome, which are caused by mutations in the tyrosine kinase domain of ROR2, patients exhibit short-limbed dwarfism characterized by abnormal morphogenesis of the face, external genitalia, and vertebral segmentation.⁴⁸⁻⁵¹ Notably, the phenotypes observed with these mutations are closely related to defects of the skeletal system, which is composed of MSC derivatives. These reports implied that the dysregulation of MSC behavior may contribute to the pathogenesis in noncanonical Wnt pathway mutants.

MSCs exhibit a number of unique cellular features, including rapid cellular proliferation, capacity to differentiate, and distinct cytoskeletal organization.^{52,53} In the present study, we found that cellular aging and related changes in gene expression were strongly associated with MSC function and were regulated by FZD5. Specifically, RECs cultured for short periods expressed high levels of FZD5 and WNT5A, whereas both genes were downregulated in RECs cultured for long periods in vitro (Figure 4A,C). The age-related protein progerin, a short isoform of lamin A (encoded by *LMNA*), is expressed in senescent fibroblasts.^{54,55} Patients with Hutchinson-Gilford progeria syndrome harbor *LMNA* mutations and exhibit abnormal osteogenesis and loss of subcutaneous adipose tissue.^{56,57} Consistent with this, the overexpression of progerin leads to the progression of osteogenic differentiation and inhibits adipogenic differentiation.⁵⁵ We found that *p16*, *progerin*, *RB1*, and *RB2* levels increased with FZD5 knockdown in RECs (Figure 4B; Figure S5A).^{58,59} Furthermore, cells with FZD5

FIGURE 5 FZD5 overexpression promotes mesenchymal stem/stromal cell (MSC) proliferation and inhibits senescence. A, MSCs were transfected with wt-FZD5 (PB513-FZD5-2xHA) and EGFP (green). Mock (PB513B-1) served as the control. B, Total (red) and HA-tagged (blue) FZD5 immunostaining in RECs transfected with PB513-FZD5-2xHA plus EGFP (green). Nuclei was visualized by Hoechst staining (blue). C, Time-dependent change in the number of overexpression (wt-FZD5) vs mock vector-transfected RECs. Bar graph shows the ratio of wt-FZD5 cells divided by Mock cell numbers. Three clones of each cell type were used (n = 3). D, DNA (1502-1522 base pairs from the 5' terminus) and amino acid (residues 501-508 from the N-terminus) sequence of wt-FZD5 and mut-FZD5. E, HA-tagged wt-FZD5 and mut-FZD5 (PB513-mut-FZD5-2xHA) in shCTRL- or shFZD5-transfected RECs (Western blot). Band intensities were quantitated and the HA-tagged FZD5/ β -actin ratios were calculated. The ratio in cells co-transfected with wt-FZD5 or mut-FZD5 and shCTRL was set to 1. F, RECs were cotransfected with shFZD5 (CS-shFZD5-EF-mRFP) and overexpression vector (wt-FZD5 or mut-FZD5). G, Ratio of REC numbers 2 weeks after shCTRL or shFZD5 transfection into wt-FZD5- or mut-FZD5-transfected cells. The mean for wt-FZD5- and shCTRL-treated cells was defined as 1; n = 4 clones. H, Adipogenic (Oil Red-O staining) and osteogenic differentiation (ALP staining) in the rescued RECs. Cells were processed for immunostaining 54 days after sorting. I, Relative expression of adipocyte (*PPAR γ* and *C/EBP β*) and osteoblast (*RUNX2* and *OSTEOCALCIN*) markers in the cells described in (H); n = 3 clones. Data represent the means \pm SEM. n.s., not significant. *P < .05, **P < .01; Student's t test

knockdown tended to have short telomere and G-tail length (Figure 4I). We found that γ H2AX expression was high in FZD5-KD RECs, which suggests that damaged DNA undergoes the repair process in these cells (Figure 4G,H).^{42,43} Based on the results of gene expression and immunostaining, the FZD5 deletion phenotype appears to change to one that resembles cellular senescence rather than one that causes aging. Like C/EBP α , C/EBP β has been reported to have the ability to induce adipocyte differentiation.⁶⁰ Especially, C/EBP β is transiently elevated early in adipocyte differentiation and play early catalytic roles in the differentiation pathway (Figure 5I).⁶¹ Thus, these findings support that FZD5/WNT5A signaling plays a role in preventing senescence in RECs, thereby preserving their potential for proliferation as immature MSCs.

The noncanonical Wnt pathway functions as a “hub” gene that coordinates stem cell functions.^{62–65} Previous reports have suggested that rheumatoid arthritis fibroblasts with high expression of Wnt5A and FZD5 acquire the characteristics of immature MSCs in vivo.⁶² MSCs with low expression of FZD5 (MECs and SECs) have osteogenic and chondrogenic differentiation capabilities similar to those of unmanipulated RECs. However, when envisaging cell transplantation, RECs with high expression of FZD5 and Wnt5A are considered to be the most appropriate cell source. An understanding—and consideration—of the properties of MSCs that can be cultured for long durations in vitro would provide insights that would enable their use in clinical research. We observed no differences in the activation of the canonical pathway among various types of MSC clones (Figure S3D). However, the differences between RECs and SECs may be explained based on the modulation of FZD5 expression. We could identify these differences in this experiment because we had analyzed a homogenous cell population originating from a single clone. The mechanism by which FZD5 exerts its effects on RECs through the noncanonical Wnt pathway remains an open question. It would be interesting to investigate if modulation of FZD5 expression can be used as a strategy for stem cell rejuvenation.

Our findings raise the possibility that aging decreases the expression of FZD5 and inhibits the response to its ligand WNT5A, thereby promoting age-related changes. The decrease in FZD5 expression is not compensated for by other signals and the positive feedback loop that induces aging cannot be interrupted until the cell cycle is arrested. These findings may contribute to the development of methods for increasing yields of full potency hMSCs, with higher capacities for proliferation and differentiation upon stimulation with appropriate growth factors, such as WNT5A or drugs that activate the noncanonical Wnt pathway.⁶⁶ In addition, such hMSCs might be purified by cell sorting using an anti-FZD5 antibody. However, the relationship between WNT5A/FZD5/ROR2 and the noncanonical Wnt pathway constitutes only one part of the complex mechanism that maintains hMSC stemness. To precisely control the behavior of hMSCs and increase their clinical utility, further studies must be conducted to characterize the pathways downstream of WNT5A/FZD5/ROR2 signaling and the detailed mechanisms of noncanonical Wnt signaling and other pathways that regulate hMSC stemness.

ACKNOWLEDGMENTS

We thank A. Kikuchi for valuable discussions and technical advice on the Wnt signaling experiment; M. Yano and K. Miura for advice;

K. Minoura for performing microarray analyses; and H. Miyoshi for constructs pENTR4-H1, CS-RfA-EG, and CS-RfA-EF-mRFP. This work was supported by the Japan Society for the Promotion of Science (JSPS) (to Seiko Harada), The Ministry of Education, Culture, Sports, Science, and Technology (MEXT) KAKENHI, Fund for the Promotion of Joint International Research (A) (Grant Number JP18KK0449), Fund for the Promotion of Joint International Research (B) (Grant Number JP19KK0216), for Scientific Research (B), (C), for Challenging Exploratory Research (Grant Number JP19K10024). Yo Mabuchi and Jun Kohyama are supported by the Japan Agency for Medical Research and Development (AMED) under grant number 18bm0404022h0001 and the Takeda Science Foundation, Japan. Core Projects on Longevity of the Keio University Global Research Institute from Keio University (to Hideyuki Okano).

CONFLICT OF INTEREST

Y. Matsuzaki is a director of PuREC, Co, Ltd. and H. Okano is a scientific consultant with SanBio, Co, Ltd., Eisai Co, Ltd., and Daiichi Sankyo Co, Ltd. The other authors declared no potential conflicts of interest.

AUTHOR CONTRIBUTIONS

S.H., Y. Mabuchi: conception and design, provision of study material or patients, collection and assembly of data, data analysis and interpretation, manuscript writing, final approval of the manuscript; J.K.: supported and supervised research, final approval of the manuscript; D.S., T.S., C.A.: data analysis and interpretation, final approval of the manuscript; S.S., M.K.: provision of study material or patients, final approval of the manuscript; Y.K., D.A.: collection and assembly of data, data analysis and interpretation, final approval of the manuscript; H.O., Y. Matsuzaki: conception and design, financial support, manuscript writing, final approval of the manuscript.

DATA AVAILABILITY STATEMENT

The data discussed in this publication have been deposited in the GEO of NCBI under accession number GSE86369. All data supporting the findings of this study are available in the article or supplementary information, or from the corresponding author upon reasonable request.

ORCID

Jun Kohyama  <https://orcid.org/0000-0001-8168-8588>

Hideyuki Okano  <https://orcid.org/0000-0001-7482-5935>

REFERENCES

1. Pittenger MF, Mackay AM, Beck SC, et al. Multilineage potential of adult human mesenchymal stem cells. *Science*. 1999;284(5411):143-147.
2. Mabuchi Y, Matsuzaki Y. Prospective isolation of resident adult human mesenchymal stem cell population from multiple organs. *Int J Hematol*. 2016;103(2):138-144.
3. Friedenstein AJ, Deriglasova UF, Kulagina NN, et al. Precursors for fibroblasts in different populations of hematopoietic cells as detected by the in vitro colony assay method. *Exp Hematol*. 1974;2(2):83-92.

4. Coutu DL, Galipeau J. Roles of FGF signaling in stem cell self-renewal, senescence and aging. *Aging (Albany NY)*. 2011;3(10):920-933.
5. Rider DA, Dombrowski C, Sawyer AA, et al. Autocrine fibroblast growth factor 2 increases the multipotentiality of human adipose-derived mesenchymal stem cells. *STEM CELLS*. 2008;26(6):1598-1608.
6. Cheng Y, Lin KH, Young TH, Cheng NC. The influence of fibroblast growth factor 2 on the senescence of human adipose-derived mesenchymal stem cells during long-term culture. *STEM CELLS TRANSLATIONAL MEDICINE*. 2020;9(4):518-530.
7. Kuilman T, Michaloglou C, Mooi WJ, Peeper DS. The essence of senescence. *Genes Dev*. 2010;24(22):2463-2479.
8. Khong SML, Lee M, Kosaric N, et al. Single-cell transcriptomics of human mesenchymal stem cells reveal age-related cellular subpopulation depletion and impaired regenerative function. *STEM CELLS*. 2019;37(2):240-246.
9. Banfi A, Muraglia A, Dozin B, Mastrogiacomo M, Cancedda R, Quarto R. Proliferation kinetics and differentiation potential of ex vivo expanded human bone marrow stromal cells: implications for their use in cell therapy. *Exp Hematol*. 2000;28(6):707-715.
10. Campisi J, d'Adda di Fagagna F. Cellular senescence: when bad things happen to good cells. *Nat Rev Mol Cell Biol*. 2007;8(9):729-740.
11. Wagner W, Horn P, Castoldi M, et al. Replicative senescence of mesenchymal stem cells: a continuous and organized process. *PLoS One*. 2008;3(5):e2213.
12. Fernandez-Rebollo E, Franzen J, Goetzke R, et al. Senescence-associated metabolomic phenotype in primary and iPSC-derived mesenchymal stromal cells. *Stem Cell Rep*. 2020;14(2):201-209.
13. Duscher D, Rennert RC, Januszkyk M, et al. Aging disrupts cell subpopulation dynamics and diminishes the function of mesenchymal stem cells. *Sci Rep*. 2014;4:7144.
14. Yukata K, Xie C, Li TF, et al. Aging periosteal progenitor cells have reduced regenerative responsiveness to bone injury and to the anabolic actions of PTH 1-34 treatment. *Bone*. 2014;62:79-89.
15. Coppe JP, Patil CK, Rodier F, et al. Senescence-associated secretory phenotypes reveal cell-nonautonomous functions of oncogenic RAS and the p53 tumor suppressor. *PLoS Biol*. 2008;6(12):2853-2868.
16. Wagner W, Ho AD. Mesenchymal stem cell preparations—comparing apples and oranges. *Stem Cell Rev*. 2007;3(4):239-248.
17. De Becker A, Riet IV. Homing and migration of mesenchymal stromal cells: how to improve the efficacy of cell therapy? *World J Stem Cells*. 2016;8(3):73-87.
18. He S, Sharpless NE. Senescence in health and disease. *Cell*. 2017;169(6):1000-1011.
19. Murphy MM, Keefe AC, Lawson JA, Flygare SD, Yandell M, Kardon G. Transiently active Wnt/beta-catenin signaling is not required but must be silenced for stem cell function during muscle regeneration. *Stem Cell Rep*. 2014;3(3):475-488.
20. Clevers H, Nusse R. Wnt/beta-catenin signaling and disease. *Cell*. 2012;149(6):1192-1205.
21. Nusse R, Clevers H. Wnt/beta-catenin signaling, disease, and emerging therapeutic modalities. *Cell*. 2017;169(6):985-999.
22. Zhang C, Chen P, Fei Y, et al. Wnt/beta-catenin signaling is critical for dedifferentiation of aged epidermal cells in vivo and in vitro. *Aging Cell*. 2012;11(1):14-23.
23. Rognoni E, Widmaier M, Jakobson M, et al. Kindlin-1 controls Wnt and TGF-beta availability to regulate cutaneous stem cell proliferation. *Nat Med*. 2014;20(4):350-359.
24. Edelberg JM, Ballard VL. Stem cell review series: regulating highly potent stem cells in aging: environmental influences on plasticity. *Aging Cell*. 2008;7(4):599-604.
25. Richter J, Traver D, Willert K. The role of Wnt signaling in hematopoietic stem cell development. *Crit Rev Biochem Mol Biol*. 2017;52(4):414-424.
26. Tilstra JS, Robinson AR, Wang J, et al. NF-kappaB inhibition delays DNA damage-induced senescence and aging in mice. *J Clin Invest*. 2012;122(7):2601-2612.
27. Chen H, Shi B, Feng X, et al. Leptin and neutrophil-activating peptide 2 promote mesenchymal stem cell senescence through activation of the phosphatidylinositol 3-kinase/Akt pathway in patients with systemic lupus erythematosus. *Arthritis Rheumatol*. 2015;67(9):2383-2393.
28. Dominici M, Le Blanc K, Mueller I, et al. Minimal criteria for defining multipotent mesenchymal stromal cells. The International Society for Cellular Therapy position statement. *Cytotherapy*. 2006;8(4):315-317.
29. Squillaro T, Peluso G, Galderisi U. Clinical trials with mesenchymal stem cells: an update. *Cell Transplant*. 2016;25(5):829-848.
30. Mabuchi Y, Morikawa S, Harada S, et al. LNGFR(+)THY-1(+)VCAM-1(hi+) cells reveal functionally distinct subpopulations in mesenchymal stem cells. *Stem Cell Rep*. 2013;1(2):152-165.
31. Mabuchi Y, Houlihan DD, Akazawa C, et al. Prospective isolation of murine and human bone marrow mesenchymal stem cells based on surface markers. *Stem Cells Int*. 2013;2013:507301.
32. Ogata Y, Mabuchi Y, Yoshida M, et al. Purified human synovium mesenchymal stem cells as a good resource for cartilage regeneration. *PLoS One*. 2015;10(6):e0129096.
33. Yasui T, Mabuchi Y, Toriumi H, et al. Purified human dental pulp stem cells promote osteogenic regeneration. *J Dent Res*. 2016;95(2):206-214.
34. Veraitch O, Mabuchi Y, Matsuzaki Y, et al. Induction of hair follicle dermal papilla cell properties in human induced pluripotent stem cell-derived multipotent LNGFR(+)THY-1(+) mesenchymal cells. *Sci Rep*. 2017;7:42777.
35. Houlihan DD, Mabuchi Y, Morikawa S, et al. Isolation of mouse mesenchymal stem cells on the basis of expression of Sca-1 and PDGFR-alpha. *Nat Protoc*. 2012;7(12):2103-2111.
36. Naka H, Nakamura S, Shimazaki T, Okano H. Requirement for COUP-TFI and II in the temporal specification of neural stem cells in CNS development. *Nat Neurosci*. 2008;11(9):1014-1023.
37. Chae WJ, Bothwell ALM. Canonical and non-canonical Wnt signaling in immune cells. *Trends Immunol*. 2018;39(10):830-847.
38. Green JL, Kuntz SG, Sternberg PW. Ror receptor tyrosine kinases: orphans no more. *Trends Cell Biol*. 2008;18(11):536-544.
39. Olson EN, Nordheim A. Linking actin dynamics and gene transcription to drive cellular motile functions. *Nat Rev Mol Cell Biol*. 2010;11(5):353-365.
40. Schlessinger K, McManus EJ, Hall A. Cdc42 and noncanonical Wnt signal transduction pathways cooperate to promote cell polarity. *J Cell Biol*. 2007;178(3):355-361.
41. Janzen V, Forkert R, Fleming HE, et al. Stem-cell ageing modified by the cyclin-dependent kinase inhibitor p16INK4a. *Nature*. 2006;443(7110):421-426.
42. Squillaro T, Antonucci I, Alessio N, et al. Impact of lysosomal storage disorders on biology of mesenchymal stem cells: evidences from in vitro silencing of glucocerebrosidase (GBA) and alpha-galactosidase A (GLA) enzymes. *J Cell Physiol*. 2017;232(12):3454-3467.
43. Alessio N, Del Gaudio S, Capasso S, et al. Low dose radiation induced senescence of human mesenchymal stromal cells and impaired the autophagy process. *Oncotarget*. 2015;6(10):8155-8166.
44. Boland GM, Perkins G, Hall DJ, Tuan RS. Wnt 3a promotes proliferation and suppresses osteogenic differentiation of adult human mesenchymal stem cells. *J Cell Biochem*. 2004;93(6):1210-1230.
45. de Boer J, Siddappa R, Gaspar C, van Apeldoorn A, Fodde R, van Blitterswijk C. Wnt signaling inhibits osteogenic differentiation of human mesenchymal stem cells. *Bone*. 2004;34(5):818-826.
46. Yamaguchi TP, Bradley A, McMahon AP, Jones S. A Wnt5a pathway underlies outgrowth of multiple structures in the vertebrate embryo. *Development*. 1999;126(6):1211-1223.
47. Takeuchi S, Takeda K, Oishi I, et al. Mouse Ror2 receptor tyrosine kinase is required for the heart development and limb formation. *Genes Cells*. 2000;5(1):71-78.

48. Robinow M, Silverman FN, Smith HD. A newly recognized dwarfing syndrome. *Am J Dis Child*. 1969;117(6):645-651.
49. Butler MG, Wadlington WB. Robinow syndrome: report of two patients and review of literature. *Clin Genet*. 1987;31(2):77-85.
50. Afzal AR, Rajab A, Fenske CD, et al. Recessive Robinow syndrome, allelic to dominant brachydactyly type B, is caused by mutation of ROR2. *Nat Genet*. 2000;25(4):419-422.
51. van Bokhoven H, Celli J, Kayserili H, et al. Mutation of the gene encoding the ROR2 tyrosine kinase causes autosomal recessive Robinow syndrome. *Nat Genet*. 2000;25(4):423-426.
52. Battula VL, Trembl S, Abele H, Bühring HJ. Prospective isolation and characterization of mesenchymal stem cells from human placenta using a frizzled-9-specific monoclonal antibody. *Differentiation*. 2008;76(4):326-336.
53. Battula VL, Bareiss PM, Trembl S, et al. Human placenta and bone marrow derived MSC cultured in serum-free, b-FGF-containing medium express cell surface frizzled-9 and SSEA-4 and give rise to multilineage differentiation. *Differentiation*. 2007;75(4):279-291.
54. Scaffidi P, Misteli T. Lamin A-dependent nuclear defects in human aging. *Science*. 2006;312(5776):1059-1063.
55. Scaffidi P, Misteli T. Lamin A-dependent misregulation of adult stem cells associated with accelerated ageing. *Nat Cell Biol*. 2008;10(4):452-459.
56. Hennekam RC. Hutchinson-Gilford progeria syndrome: review of the phenotype. *Am J Med Genet A*. 2006;140(23):2603-2624.
57. Burtner CR, Kennedy BK. Progeria syndromes and ageing: what is the connection? *Nat Rev Mol Cell Biol*. 2010;11(8):567-578.
58. Alessio N, Bohn W, Rauchberger V, et al. Silencing of RB1 but not of RB2/P130 induces cellular senescence and impairs the differentiation potential of human mesenchymal stem cells. *Cell Mol Life Sci*. 2013;70(9):1637-1651.
59. Helmbold H, Komm N, Deppert W, et al. Rb2/p130 is the dominating pocket protein in the p53-p21 DNA damage response pathway leading to senescence. *Oncogene*. 2009;28(39):3456-3467.
60. Farmer SR. Transcriptional control of adipocyte formation. *Cell Metab*. 2006;4(4):263-273.
61. Yeh WC, Cao Z, Classon M, McKnight SL. Cascade regulation of terminal adipocyte differentiation by three members of the C/EBP family of leucine zipper proteins. *Genes Dev*. 1995;9(2):168-181.
62. Sen M, Lauterbach K, El-Gabalawy H, et al. Expression and function of wingless and frizzled homologs in rheumatoid arthritis. *Proc Natl Acad Sci USA*. 2000;97(6):2791-2796.
63. Thiele S, Zimmer A, Gobel A, et al. Role of WNT5A receptors FZD5 and RYK in prostate cancer cells. *Oncotarget*. 2018;9(43):27293-27304.
64. Wang X, Tang P, Guo F, et al. mDia1 and Cdc42 regulate activin B-induced migration of bone marrow-derived mesenchymal stromal cells. *STEM CELLS*. 2019;37(1):150-162.
65. Yu F, Wu F, Li F, et al. Wnt7b-induced Sox11 functions enhance self-renewal and osteogenic commitment of bone marrow mesenchymal stem cells. *STEM CELLS*. 2020;38(8):1020-1033.
66. Mehdawi LM, Prasad CP, Ehrnstrom R, et al. Non-canonical WNT5A signaling up-regulates the expression of the tumor suppressor 15-PGDH and induces differentiation of colon cancer cells. *Mol Oncol*. 2016;10(9):1415-1429.

SUPPORTING INFORMATION

Additional supporting information may be found online in the Supporting Information section at the end of this article.

How to cite this article: Harada S, Mabuchi Y, Kohyama J, et al. FZD5 regulates cellular senescence in human mesenchymal stem/stromal cells. *Stem Cells*. 2021;39:318-330. <https://doi.org/10.1002/stem.3317>